Energy Conversion and Management 158 (2018) 81–91

Contents lists available at ScienceDirect

Energy Conversion and Management

journal homepage: www.elsevier.com/locate/enconman

Degradation based operational optimization model to improve the productivity of energy systems, case study: Solid oxide fuel cell stacks

Tarannom Parhizkar[a,*], Saeedreza Hafeznezami[b]

[a] Department of Energy Engineering, Sharif University of Technology, Tehran, Iran
[b] Department of Civil and Environmental Engineering, UCLA, Los Angeles, CA 90095, USA

ARTICLE INFO

Keywords:
Degradation based optimization
Solid oxide fuel cell
Productivity
Operating conditions
Target lifetime

ABSTRACT

In the present study a comprehensive thermodynamic model and degradation based optimization framework for energy management of anode supported solid oxide fuel cell (SOFC) stacks are carried out. The optimization framework determines optimum operating conditions to maximize system productivity (energy generation over system lifetime) considering degradation mechanisms. The main degradation mechanisms in anode supported SOFCs are nickel coarsening and oxidation. In this study, the optimum operating conditions regarding these degradation mechanisms to achieve maximum productivity at different target lifetimes are derived. The results show that target lifetime has a significant impact on system productivity and optimum operating temperature and current density. Furthermore, SOFC optimum operating conditions as a function of target lifetime are derived. To show the effectiveness of the developed framework, model outputs are compared with two other operating strategies; a base case strategy that optimizes system operating conditions without considering degradation mechanisms and a strategy based on Department of Energy's (DOE) 2016 fuel cell report. Results illustrated that degradation based optimization is more beneficial for improving the entire performance in long-term operation. For instance, system productivity is 7.4% higher in comparison with DOE strategy during 40,000 h operating lifetime. It is expected that the proposed methodology will lead to more rapid commercialization of SOFC technology.

1. Introduction

The solid oxide fuel cell (SOFC) is entirely solid-state and highly efficient. It has many advantages as a power generation device. For instance, it produces no noise during operation since it has no moving parts. In addition, the SOFC has no strict requirements on fuel gas composition. Unlike some other types of fuel cells that need pure hydrogen, the SOFC can use variety of fuels, most of which are hydrocarbon-based fuels such as methane and propane. The other advantage is that since SOFC operates at high temperatures, usually between 500 °C and 1000 °C, expensive platinum catalyst is not required. Also, the heat generated during operation can be used as a source of heat energy such as heating buildings [1]. However, due to issues caused by contaminants and degradation mechanisms over the long term, SOFCs are still not broadly implemented [2]. Thus, a fundamental understanding of degradation mechanisms for long term analysis of SOFC system is needed. Several studies have been conducted in recent years that model degradation mechanisms and the effect of degradation on performance deterioration [3–5]. For instance, in [6], a novel prediction approach for proton exchange membrane fuel cell performance deterioration is proposed based on a multi-physical aging model with particle filter approach. Optimizing operating conditions with considering performance deterioration leads to more accurate and reliable results [7,8].

In this study, a degradation based optimization (DBO) framework is proposed [9], and optimum operating conditions are derived in order to advance the commercialization of SOFCs.

Degradation based optimization is a model that accounts for system degradation mechanisms in the optimization procedure. The goal of the DBO is to derive the optimum operating conditions or design parameters of the system to maximize or minimize a specific objective function. In energy engineering systems, the optimum operating conditions mostly result in minimizing the system total cost or maximizing the system energy production through system operating lifetime [10,11].

There is a significant body of research that has focused on SOFC optimization models [12]. In most studies the optimization strategies are different. In addition, they are optimizing either operating

* Corresponding author.
E-mail addresses: Parhizkar@seri.sharif.edu (T. Parhizkar), Saeedreza@ucla.edu (S. Hafeznezami).

https://doi.org/10.1016/j.enconman.2017.12.045
Received 23 August 2017; Received in revised form 8 December 2017; Accepted 12 December 2017

Nomenclature

A	area, m^2
c_{O_2}	gas-phase concentration of O_2, mol m^{-3}
D	mass diffusivity, $m^2 s^{-1}$
E	activation energy, kJ mol^{-1}
F	Faraday's constant, C $equiv^{-1}$
H	enthalpy, J mol^{-1}
i	current density, A m^{-2}
I	working current, A
k_{ox}	rate constant for oxidation reaction, $m^3 kg^{-1} s^{-1}$
$k_{s,cap}$	nickel particles growth rate
L	length, m
M	molecular weight, kg mol^{-1}
n	equivalent electron per mole of reactant, equiv mol^{-1}
ni	number of nickel particles, mol
p	pressure, Pa
P	dimensionless pressure
pr	site occupation probability
R	universal gas constant, J $mol^{-1} K^{-1}$
r	nickel particles radius
r_{ox}	rate of oxidation, mol $kg^{-1} s^{-1}$
S^0	standard entropy, J $mol^{-1} K^{-1}$
T	temperature, K
TPB	triple phase boundary, m m^{-3}
u	decision variable
v	voltage, V
V_{Ni}	nickel particles volume
x	state variable
X	molar fraction of component in the mixture
β	Ohmic resistance, Ω
η	overpotential, V
σ	electrical conductivity, $\Omega^{-1} m^{-1}$
ϕ	porosity
ψ	tortuosity
ν	diffusion volume of simple molecules, cm^3
α	fraction of the reaction heat that is generated at the anode
δ	pre-exponential factor, $\Omega^{-1} m^{-2}$
θ_O	bulk oxygen coverage, dimensionless
γ	exponential activity parameter, kJ mol^{-1}
τ	perimeter

Subscript and super script

0	initial condition
1	bipolar plate (interconnect)
2	fuel channel
3	anode
4	electrolyte
5	cathode
6	air channel
Act	activation
ch	channel
Conc	concentration
Ohm	Ohmic
Opt	optimal
x	x direction
y	y direction
z	z direction

conditions or design parameters [13]. For instance, Feng et al. [14] developed a design optimization model to maximize system output power. In this study, the structure of a single tubular SOFC is considered as a decision variable. Results show that optimum structure leads system to operate at 18.2% higher output power in comparison with not-optimized structure design. Duhn et al. [15] proposed a novel optimization model to determine the optimal geometric flow design. The modeling of the system is based on the computational fluid dynamic modeling and decision variables are the channels width and the area in front of the parallel channels. The optimal design maximizes flow uniformity index which is directly proportional to the maximum obtainable overall conversion. Hasanabadi et al. [16] investigated a model to optimize the microstructure design of an SOFC. In their study two-point correlation functions are used to realize the three dimensional porous microstructure of the SOFC. The results show that the optimization procedure can be used as a robust tool to design the optimal microstructure.

In [17] a multi-objective optimization model is investigated that optimizes operating conditions of a tri-generation system driven by SOFC. In this study the objectives of the optimization are to minimize system total product unit cost and maximize exergy efficiency, simultaneously. The optimization algorithm is based on genetic algorithm and results indicate that optimal conditions are on the Pareto front. In [18], the operating conditions of a tri-generation system is optimized to make the system economically affordable while meeting the whole cooling demand and 50% of the total electricity demand. The model is optimized for a tri-generation system includes 50 kW tubular SOFC combined with heat recovery steam generator, combustion chamber and a chiller. Results show that optimal operating conditions lead system to be economically affordable and have an approximately net annual profit of $874,200.

The design parameters and operating conditions can be optimized more accurately by considering degradation mechanisms in the optimization procedure [19]. Xu et al. [20] developed an optimization model considering system degradation to optimize thermal stress performance of the SOFC. The aim of the model in their study is predicting the thermal stress of an anode-supported SOFC for different designs. A three dimensional thermal stress model is considered as the degradation mechanism. The results show that as the interconnect area increases, the thermal stress decreases. In addition, the thermal stress of the counter-flow and co-flow are similar.

As is clear from reviewed literature, most SOFC degradation models are based on experimental data. However, in principle-based models, the degradation mechanisms rate dependency to operating conditions and SOFC material properties can be determined more accurately.

As can be seen, in the case of SOFC optimization models, significant research has been done in the last decade [21–24]. However, there is not many studies that optimize system considering degradation [25–28]. The main contributions of the present study are as follow:

- One of the main novelties of the proposed framework is the consideration of degradation model in the optimization procedure. The degradation mechanism can result in performance system long term productivity deterioration. The rate of degradation mechanism depends on system operating conditions. Effective control of degradation mechanism rate is a key element of the efficient operation of energy systems. The proposed model manages degradation mechanism by optimizing system's operating conditions in order to maximize lifetime productivity.
- An improved degradation based optimization approach is used in order to address degradation mechanism effect on system productivity deterioration. This new approach results in more accuracy in long term simulation and more reliable and realistic optimal operating conditions.
- The proposed framework produces optimal operating conditions of SOFC stacks to achieve maximum productivity over system target

lifetime.

- The optimal operating conditions as a function of target lifetimes are derived in order to maximize system lifetime productivity.
- In addition, a 150 kW SOFC power plant is modeled as a case study, and the optimal operating condition is derived. Results show the effectiveness of the proposed model and solution algorithm.

For this purpose, a brief overview of the developed degradation based optimization framework is presented in Section 2. The formulation of SOFC degradation based optimization is presented in Section 3, and the sub modules are introduced. Results are presented in Section 4 and finally the study is concluded with an overall discussion on the advantage of DBO framework development in Section 5.

2. Generic problem statement

Degradation mechanisms deteriorate system productivity over long term operation. On the other hand, degradation mechanisms rate is a function of operating conditions. Therefore, productivity deterioration over long term operation can be controlled by optimizing system operating conditions. As mentioned before, DBO model optimizes system operating conditions with considering degradation effects in the modeling. This model has two main components. Firstly, it studies the dependency of degradation mechanisms rate to the operating conditions. And secondly, it considers degradation mechanisms effect on system long term productivity (Fig. 1).

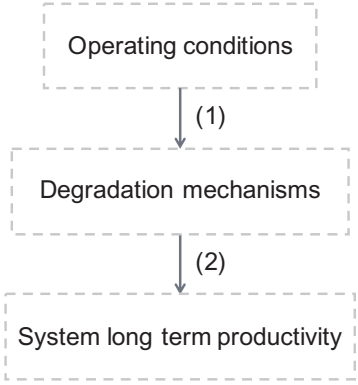

Fig. 1. Two main parts of DBO model.

In order to consider these two main components in the optimization model, system process, degradation and optimization modules should be developed. These three modules are integrated and solved concurrently.

The process module is an Input/output (I/O) model of the system which formulates the dependency of system outputs such as performance to the system inputs like ambient and operating conditions.

The degradation module can be developed based on the degradation mechanisms governing equations and available data.

The optimization module, consists of an objective function and several constraints. The objective function shows the operator strategy of operation. In this study, maximizing power generation is the objective of the operation optimization, and the constraints consider the operation and economical limitations of the system.

The geometric feature of the studied SOFC is illustrated in Fig. 2, which includes external dimensions (L_X, L_Y, and L_Z) and individual layers' thicknesses (L_i).

The DBO model of a SOFC stack consists of process, degradation, and optimization modules. In the process module, system output power

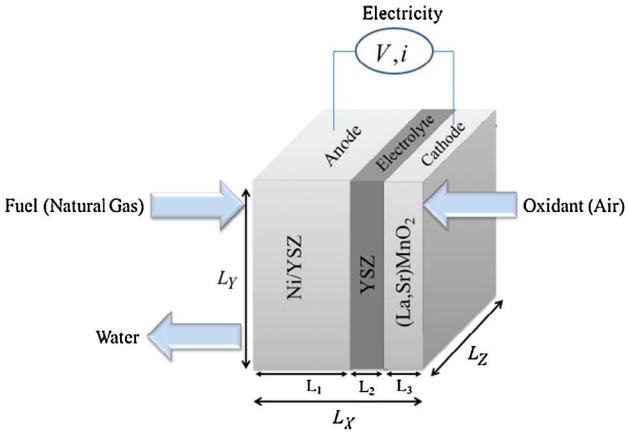

Fig. 2. 3D configuration of a planar SOFC single cell.

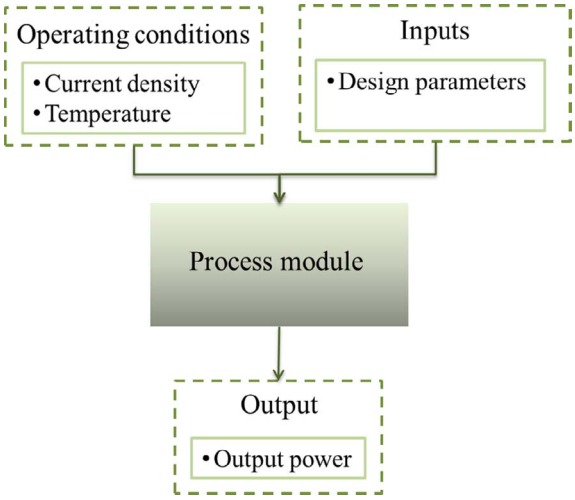

Fig. 3. Flow diagram of a SOFC process module.

as a function of operating conditions (cell temperature and current density) and design parameters is derived. The data flow diagram of the process model is presented in Fig. 3.

The second module is degradation module that models the main degradation mechanisms including nickel coarsening and oxidation of SOFC stack. In this module, degradation rate of catalyst layer is calculated at different operating conditions. In addition, the effect of degradation mechanisms on stack design parameters deterioration such as triple phase boundary and conductivity is determined.

System performance deterioration as a function of operating conditions can be calculated by integrating process and degradation modules. The data flow diagram of the integrated model is presented in Fig. 4. At each time step, degraded design parameters are derived from degradation module. The degraded design parameters are used as updated inputs of the modules for the next time step.

The third module is the SOFC optimization module. In this module, operating conditions are optimized in order to maximize system lifetime productivity. The objective function of optimization model is maximizing lifetime productivity and the decision variables are the operating conditions. Optimization model constraints are derived from process and degradation modules. The data flow diagram of SOFC DBO model (integration of process, degradation and optimization modules) is presented in Fig. 5.

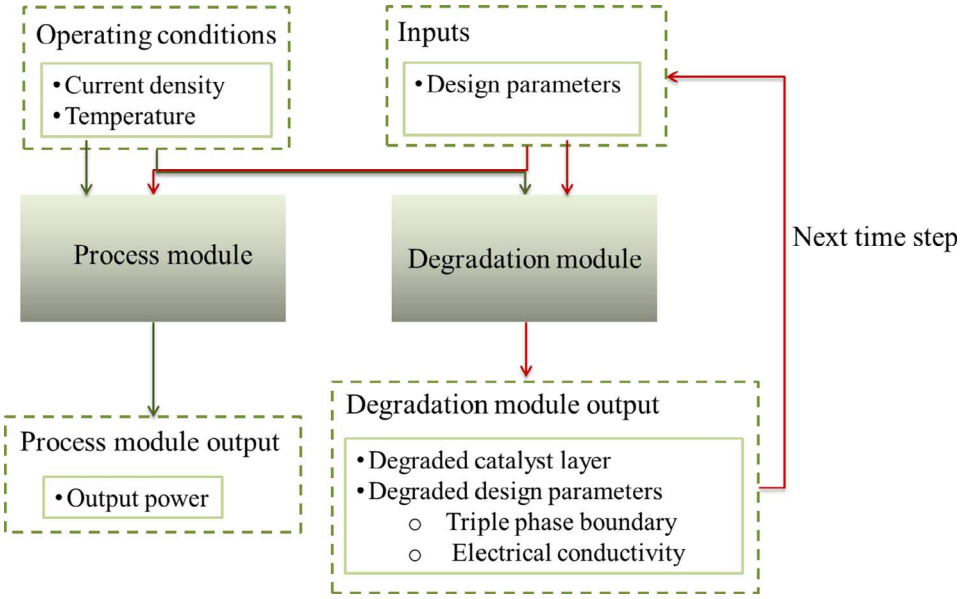

Fig. 4. Flow diagram of SOFC integrated process and degradation modules.

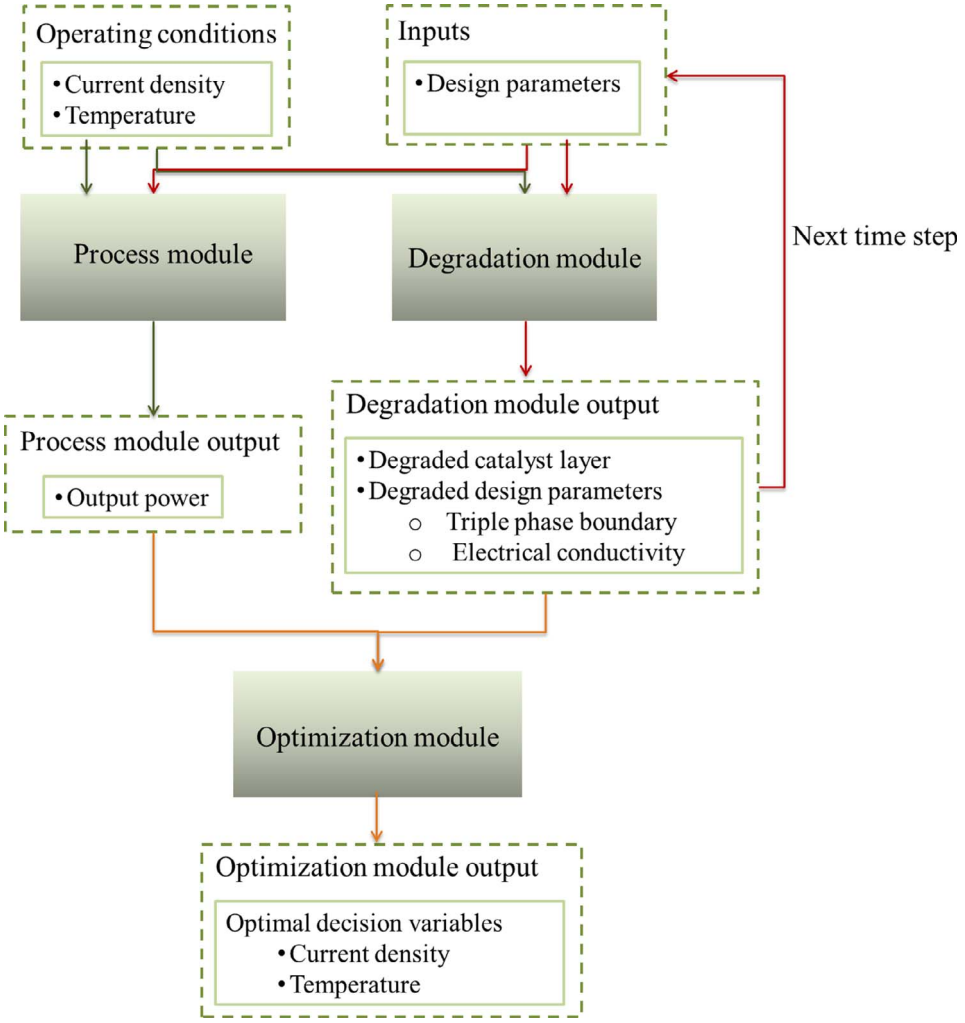

Fig. 5. Flow diagram of SOFC DBO model.

3. Degradation based optimization model

3.1. SOFC process module

The flow diagram of process module is presented in Fig. 6. Inputs and operating conditions are applied to the voltage calculation sub-module and system output power is derived based on the governing equations presented in this section.

The main governing equation is the actual operating potential evaluation (V), (Eq. (1)). This term is derived from the open circuit potential (V_{OCV}) by considering occurred losses include: Ohmic (η_{ohm}), concentration (η_{conc}) and activation (η_{act}) over potentials [24,25].

$$V(t) = V_{OCV} - \left(\sum_{j} \eta_{ohm,j}(t) + \eta_{conc,3}(t) + \eta_{conc,5} + \eta_{act,3}(t) + \eta_{act,5}\right) \quad j = 1,3,4,5 \tag{1}$$

The open circuit potential is estimated by Eq. (2) [24,25].

$$V_{OCV} = \frac{-\left(H_{H_2O} - H_{H_2} - \frac{1}{2}H_{O_2}\right) + T \times \left(S^o_{H_2O} - S^o_{H_2} - \frac{1}{2}S^oO_2\right) - RTln\left[\frac{P_{H_2O}}{P_{H_2}(P_{O_2})^{\frac{1}{2}}}\right]}{2F} \tag{2}$$

The Ohmic overpotential is calculated based on the Ohmic law. The Ohmic overpotential of interconnect and electrolyte are calculated as Eq. (3) [24,25].

$$\eta_{ohm,j} = I\beta_j \quad j = 1,4 \tag{3}$$

This loss depends on the electrical resistances of interconnect (β_1) and electrolyte (β_4) which are calculated from Eqs. (4) and (5) [24,25].

$$\beta_1 = \frac{L_1}{L_y L_z \sigma_1} + \frac{L_2}{(1+n_{ch})L_t L_y \sigma_1} + \frac{L_6}{(1+n_{ch})L_t L_z \sigma_1} \tag{4}$$

$$\beta_4 = \frac{L_4}{L_y L_z \sigma_4} \tag{5}$$

Moreover, the ohmic overpotential of cathode and anode are calculated as Eq. (6) [24,25].

$$\eta_{ohm,j}(t) = \frac{I(A_{j,opt}(t) - L_y L_z)L_{j,opt}(t)}{2A_{j,opt}(t)L_y L_z(1-\phi_j)\sigma_4} + \frac{I(Lj - L_{j,opt}(t))}{L_y L_z(1-1.8\phi_j)\sigma_i(t)} \quad j = 3,5 \tag{6}$$

In the Eq. (6), the area of the active TPB regions ($A_{j,opt}$) and average diameter of electrodes parallel ports ($D_{P,j}$) are calculated as follow [24,25].

$$A_{j,opt}(t) = (1 + 2L_{j,opt}(t)/D_{p,j})L_{yz} \tag{7}$$

$$D_{P,j} = D_{W,j}\Phi_j/(1-\Phi_j) \tag{8}$$

The concentration over potentials in the cathode and anode layers are given by Eqs. (9) and (10), respectively [24,25].

$$\eta_{conc,5} = \frac{RT}{4F}\ln\left(\frac{P_{O_2}}{P_{O_2,TPB}}\right) \tag{9}$$

$$\eta_{conc,3}(t) = \frac{RT}{4F}\ln\left(\frac{P_{H_2}P_{H_2O,TPB}(t)}{P_{H_2O,TPB}(t)P_{H_2O}}\right) \tag{10}$$

The required partial pressure of water ($P_{H_2O,TPB}$), partial pressure of hydrogen ($P_{H_2,TPB}$), partial pressure of oxygen ($P_{O_2,TPB}$), mass diffusivity at anode (D_3) and cathode side (D_5) for calculating concentration overpotentials are obtained from Eqs. (11–15) [24,25].

$$P_{H_2O,TPB}(t) = p_f X_{H_2O} + \frac{RT\psi_3}{2FD_3(t)\phi_3}\frac{L_3 I}{L_y L_z} \tag{11}$$

$$P_{H_2,TPB}(t) = p_f X_{H_2} - \frac{RT\psi_3}{2FD_3(t)\phi_3}\frac{L_3 I}{L_y L_z} \tag{12}$$

$$P_{O_2,TPB} = p_{air} - (p_{air} - X_{O_2}p_{air})\exp\left(\frac{RT\psi_5 L_5 I}{4FD_5\phi_5 p_{air}L_y L_z}\right) \tag{13}$$

$$D_3 = \frac{1.43\times10^{-7}T^{1.75}(M_{H_2}+M_{H_2O})^{\frac{1}{2}}}{p_f\left(2M_{H_2}M_{H_2O}\right)^{\frac{1}{2}}\left(v_{H_2}^{\frac{1}{3}} + v_{H_2O}^{\frac{1}{3}}\right)^2} \tag{14}$$

$$D_5 = \frac{1.43\times10^{-7}T^{1.75}(M_{O_2}+M_{N_2})^{\frac{1}{2}}}{p_{air}\left(2M_{O_2}M_{N_2}\right)^{\frac{1}{2}}\left(v_{O_2}^{\frac{1}{3}} + v_{N_2}^{\frac{1}{3}}\right)^2} \tag{15}$$

The last over potential is activation which is given by Eq. (16), where $i_{0,j}$ stand for the exchange current densities and are calculated from Eq. (17) [24,25].

$$\eta_{act,j}(t) = \frac{RT}{\alpha nF}\sinh^{-1}\left(\frac{i}{i_{0,j}(t)}\right) \quad j = 3,5 \tag{16}$$

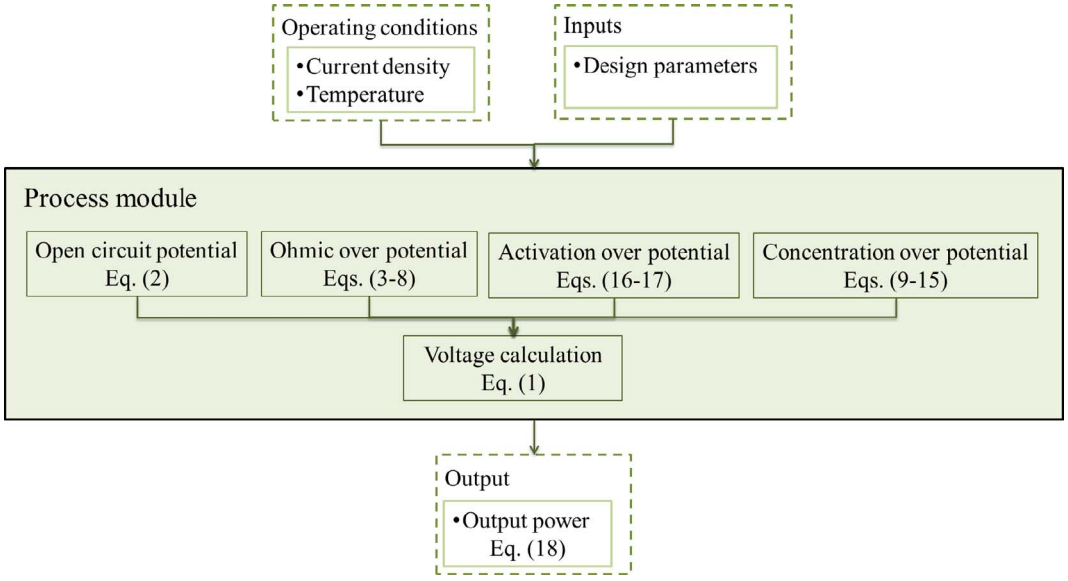

Fig. 6. Detailed data flow diagram of a SOFC process module.

$$i_{0,j}(t) = \frac{RT}{nF} k \exp\left(-\frac{E_j}{RT}\right) \quad j = 3,5 \tag{17}$$

Based on the calculated actual operating potential (Eq. (1)), the electrical power density of SOFC is obtained by the multiplication of the actual operating potential and current density as represented in Eq. (18).

$$Power_d(t) = V(t) \times i \tag{18}$$

3.2. SOFC degradation module

As system operates, different degradation mechanisms occur. The case being studied is an anode supported SOFC stack with stationary application. The main degradation mechanisms in anode supported SOFCs are nickel coarsening and oxidation which occur at the anode side. Nickel phase in the yttria-stabilized zirconia (YSZ) structure will be reformed in unsuitable operating conditions. Nickel particle size increases in this undesired reformation mechanism. Moreover, nickel will be oxidized in the presence of oxygen, water and oxygen ions at anode side. The increase in nickel particle size and nickel oxidation, diminish the contact of reactants within the Ni phase. Therefore, the triple phase boundary and the electronic conductivity are degraded [27–30].

Based on the degradation reactions, the flow diagram of degradation module is presented in Fig. 7. The model is run at each time step and parameters are updated for the subsequent time step. At the beginning of each time step, inputs and operating conditions are applied to the governing equations of degradation module and nickel coarsening and oxidation rate are derived. The rate of these two degradation mechanisms determine remaining catalyst active surface area. As a result, degraded design parameters including triple phase boundary and electrical conductivity are calculated. These values are the updated design parameters, and are the inputs of the next time step.

As can be seen in Fig. 7, nickel coarsening and nickel oxidation are the two main sub-modules of degradation module. Tanasini et al. [31] developed a nickel coarsening model, in which particle coarsening obeys charging capacitor law as Eq. (19).

$$R(t) = (R(\max) - R(0))[1 - \exp(-k_{s,cap} t)] + R(0) \tag{19}$$

$R(t)$ is nickel radius at time t. $R(\max)$ and $R(0)$ are maximum and initial radius of nickel particles. And, $k_{s,cap}$ is the capacitor constant. According to mass balance of nickel particles on catalyst layer, number of remaining nickel particles can be calculated as Eq. (20).

$$ni_c(t) = \left(\frac{R(0)}{R(t)}\right)^3 \times ni(0) \tag{20}$$

Moreover, nickel can be oxidized by the presence of oxygen or water vapor at anode side [26].

$$Ni + \frac{1}{2}O_2 \leftrightarrow NiO \tag{c}$$

$$Ni + H_2O \leftrightarrow NiO + H_2 \tag{d}$$

To evaluate the oxidation rate of each reaction, mole fraction of O_2, and H_2O at anode side should be determined. The amount of H_2O depends on input fuel and oxidant. However, oxygen can exist at the anode side because of leakage or water electrolysis [27,28]. The nickel oxidation rate is calculated as Eq. (21).

$$r_{ox} = \frac{dni(t)}{dt} = k_{ox} c (1 - \theta_o)^2 \tag{21}$$

Where k_{ox} is the reaction rate coefficient and calculated as Eq. (22).

$$k_{ox} = k' \exp\left(-\frac{E_{ox}}{RT}\right) \exp\left(-\frac{\gamma}{RT}\theta_o\right) \tag{22}$$

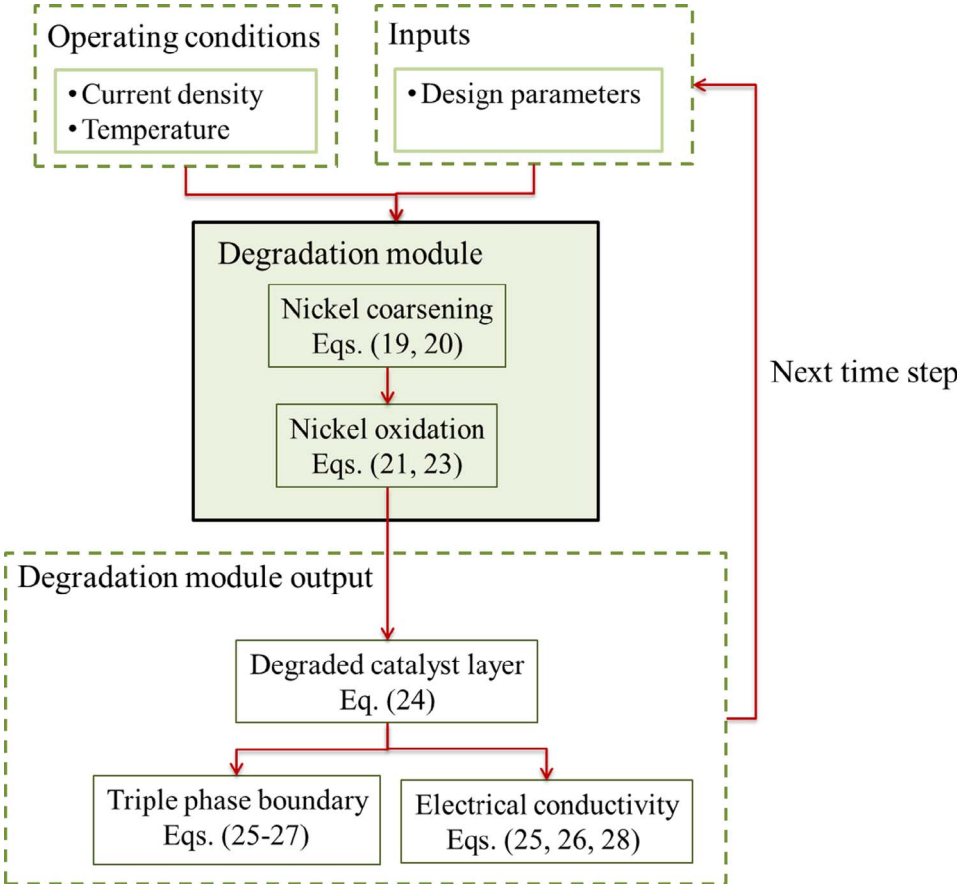

Fig. 7. Detailed data flow diagram of a SOFC degradation module.

The remaining nickel particles is calculated as Eq. (23).

$$ni(t) = ni_c(t) - \int_0^t r_{ox}.\, dt \tag{23}$$

In this equation, $ni_c(t)$ is the remained nickel particles with considering coarsening mechanism. The available active surface area of catalyst layer is corresponding to available nickel particle surface area that is calculated as Eq. (24)

$$A(t) = k_A \times ni(t) \times 4\pi R(t)^2 \tag{24}$$

In addition, nickel coarsening and oxidation decrease occupation probability and as a result affect the available nickel particles.

$$\frac{pr(t)}{pr_c} = \frac{A(t)}{A(0)} \tag{25}$$

$$\tau_{Ni}(t) = ni(t)\left(\frac{1-pr(t)}{pr(t)}\right) + 3.6ni(t)^{0.5} \tag{26}$$

And finally, triple phase boundary and electrical conductivity of SOFC are calculated as Eqs. (27), (28), respectively [29].

$$TPB(t) = 2[(\pi - 2\theta)r(t)]\tau_{Ni}(T) \tag{27}$$

$$\sigma_{eff}(t) = \sigma_0(\tan\theta)[pr(t) - pr_c]^{1.3} \tag{28}$$

In these equations, $r(t)$, $\tau_{Ni}(t)$ and $pr(t)$ are degraded over the operating lifetime and as a result triple phase boundary and electrical conductivity deteriorate over time. These deteriorated parameters are the input of process and optimization modules.

3.3. SOFC optimization module

The optimization objective is to maximize total power generation through system lifetime (productivity) with considering degradation mechanisms.

The fuel cell stack is the most expensive component with a higher failure rate in comparison with other components of a SOFC power plant [32]. Therefore, a complete replacement of the stack is considered as system target lifetime and it is assumed that other components can be maintained or replaced with a low cost during stack operation [32,33]. In addition, it is assumed that the operating condition of the SOFC power plant components are independent.

As a result, in this study, the main part of the power plant which is SOFC stack is studied and optimal operating conditions of the stack is derived.

Decision variables of the optimization model are the operating conditions of the stack which are cell temperature and current density. The optimization module flow diagram is presented in Fig. 8.

The objective function is presented as Eq. (29).

$$\max J[u(t), x(t)] = \int_t^{t+T} Power(t)d\tau \tag{29}$$

$Power(t)$ is the SOFC output power which here is as Eq. (30).

$$Power(t) = V(t) \times i \times A(t) \tag{30}$$

$V(t)$ and $A(t)$ are the actual operating potential and active surface area which are derived based on process and degradation modules. The optimization constraints set includes restrictions on the system operation. For instance, the operating temperature and current density ranges are considered. Moreover, it is assumed that SOFC operates up to half of the nickel degraded [34].

To solve the proposed degradation based optimization model, the genetic algorithm (GA) method is used [35]. The GA algorithm starts from a population of randomly generated individuals (operating conditions) and occurs in generations. In each generation, the optimization output (productivity) is calculated, and the fitness of every individual in the population is evaluated. Multiple individuals are selected from the current population (based on their fitness), and modified to form a new population. The new population is used as an initial value in the next iteration of the algorithm. The loop is repeated until the required number of iterations yield the same optimal results.

4. Results and discussion

4.1. Case study

As a case study, a 150 kW SOFC is selected. Properties and constant values used in the simulations are referenced from Wen et al. [25] research and are presented in Table 1.

4.2. Validation

The model should be validated before it is applied to the case study. Two steps of validation are performed to illustrate that results are reliable. In the first step, to validate the SOFC process module, comparison between model outputs with results published by Wen et al. [25] is performed. Fig. 9 illustrates that under the same SOFC geometric dimensions and operating condition (1073 K), the general shape of two polarization curves are similar.

According to the results, the absolute error varies between 0 and 5%. If the purpose of the simulation model was to have an as accurate model as possible, this might have been problematic, but in this case our focus is to use the model for operation optimization, and deriving an accurate parameters trend is sufficient, which is accurately achieved.

In the second step, the integration of SOFC degradation and process modules is validated. The voltage degradation rate at different current densities is used to validate this integrated model. As mentioned before, the main degradation mechanisms in anode supported SOFCs occur at anode side. Therefore, the integrated model results are compared with Muller et al. [36] experimental research that studies anode degradation mechanisms. In [36], the efficiency and long term stability of Ni-YSZ anodes as a function of current density are studied for various SOFC single cells. Tables 2 and 3, compare experimental data gathered by Muller et al. [36] with modeling results at two different operating current densities representing the low and high ranges of operations.

Comparison at low current density range, shows that the voltage degradation rate is slightly higher in the simulation than what is measured.

In addition, the absolute error at higher current densities is greater due to the existence of other degradation mechanisms such as cathode degradations which are ignored in the modeling.

Improvements in the agreement between the simulations and experimental data can be obtained by modeling all degradation mechanisms such as cathode degradation mechanisms. However, the main objective of the present study is to capture degradation profile over time which is achieved with enough accuracy.

4.3. Optimal operating points

Solid oxide fuel cell operating conditions (temperature and current density) have a great impacts on power deterioration over time. SOFC can operate at operating temperature range of 873–1123°K [37]. And, the current density ranges of 1–10 A/cm^2 [38].

In order to maximize system power generation through lifetime, the optimum operating conditions should be determined. In addition, system target lifetime affect the optimum values. In this study, optimum operating conditions are determined based on the developed DBO model for different target lifetimes.

The optimized operating conditions and power generation through time according to the three target lifetimes are shown in Fig. 10. When the target operating time is 10,000 h, the initial power is 136.5 kW at the optimum temperature and current density of 1065.2 K and 2.69 A/cm^2, respectively. As target lifetime increases, the initial power and optimal operating conditions decrease. For instance, at 40,000 h target

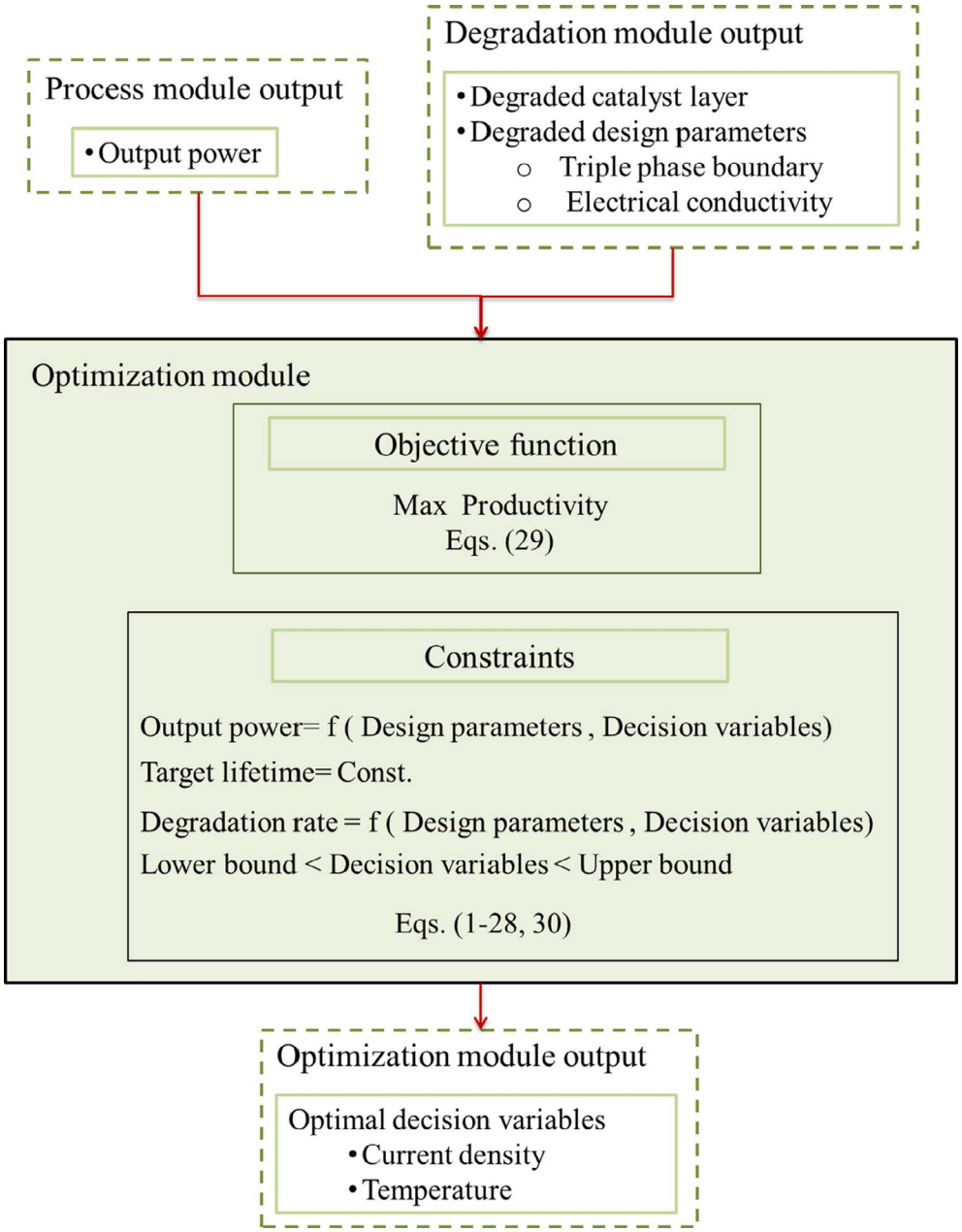

Fig. 8. Detailed data flow diagram of SOFC optimization module.

Table 1
Physical and chemical properties of the studied SOFC stack.

Parameter	Value	Parameter	Value
A	100 cm^2	σ_4	$33.4 \times 10^3 \exp(-10.3 \times 10^3/T)\ \Omega^{-1} m^{-1}$
n_f	1000	σ_5	$8.4 \times 10^3\ \Omega^{-1} m^{-1}$
$D_{W,3}$	14×10^{-6} m	Ψ_3	9.5
$D_{W,5}$	14×10^{-6} m	Ψ_5	7.2
E_3	$140 \times 10^3\ J\ mol^{-1}$	L_1	0.05 cm
E_5	$137 \times 10^3\ J\ mol^{-1}$	L_2	0.1 cm
n_{ch}	10	L_3	0.05 cm
α	0.5	L_4	0.002 cm
δ_3	$6.54 \times 10^{11}\ \Omega^{-1} m^{-2}$	L_5	0.005 cm
δ_5	$2.35 \times 10^{11}\ \Omega^{-1} m^{-2}$	L_6	0.1 cm
ν_{O_2}	16.3 cm^3	L_{ch}	0.2 cm
ν_{H_2}	6.12 cm^3	L_t	0.8 cm
ν_{H_2O}	13.1 cm^3	L_y	10 cm
ν_{N_2}	18.5 cm^3	L_z	10 cm
σ_1	$1.5 \times 10^6\ \Omega^{-1} m^{-1}$	$L_{3,opt}$	3.75×10^{-4}
σ_3	$8.0 \times 10^4\ \Omega^{-1} m^{-1}$	$L_{5,opt}$	7.20×10^{-4}

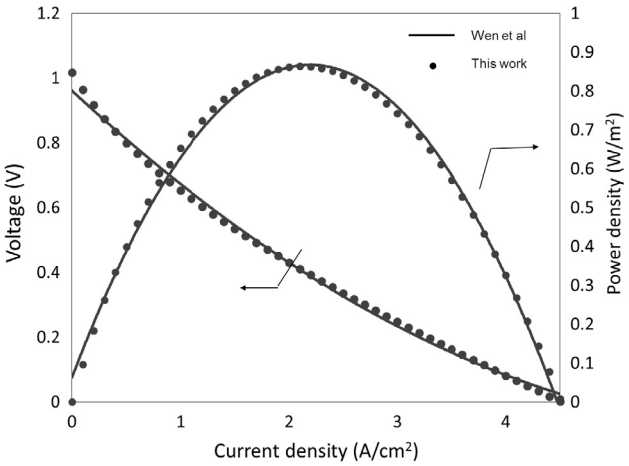

Fig. 9. Comparison between Wen et al. [25] results and model output at 1223 K.

Table 2
Comparison between experimental data and modeling results at low current density.

Current density (A/cm^2)	Anode voltage degradation rate (V/1000 h)		Differences (V/1000 h)
	Experimental data	Modeling results	
0.2	0.032	0.039	+0.007

Table 3
Comparison between experimental data and modeling results at high current density.

Current density (A/cm^2)	Anode voltage degradation rate (V/1000 h)		Differences (V/1000 h)
	Experimental data	Modeling results	
0.52	0.057	0.047	−0.01

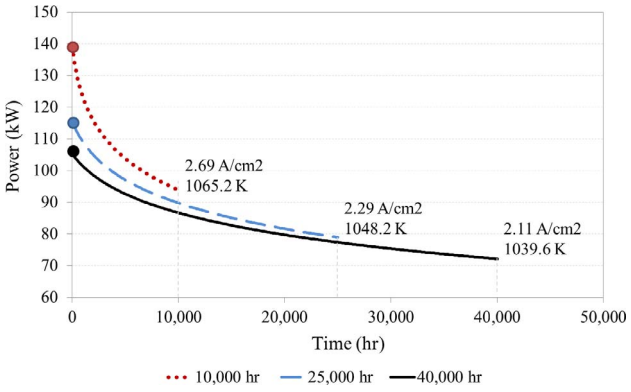

Fig. 10. Power profile over time at three target lifetimes.

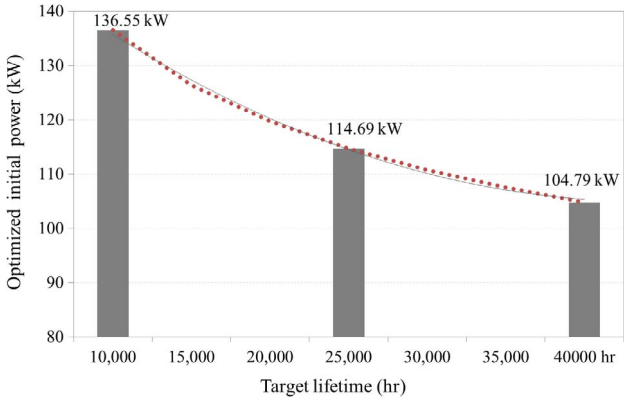

Fig. 11. Optimized initial power at different target lifetimes.

operating time, the initial power is 114.7 kW at optimum temperature and current density of 1039.6 K and 2.11 A/cm^2, respectively. These results suggest that the operating conditions should be decreased for long term operation but increased if the expected lifetime is shorter. In other words, increasing temperature and current density are more beneficial for improving the entire performance in short-term operation.

Fig. 11 presents the optimum initial power at different target lifetimes. As is clear, at higher target lifetime, system operates at lower optimum initial power because of lower degradation rate in this range of power.

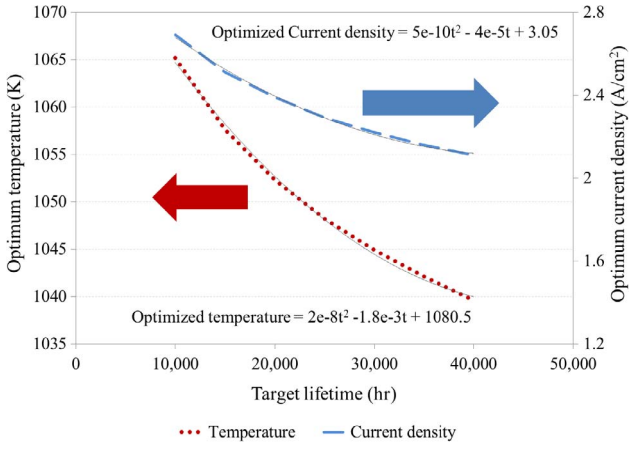

Fig. 12. Optimum operating conditions as a function of target lifetime.

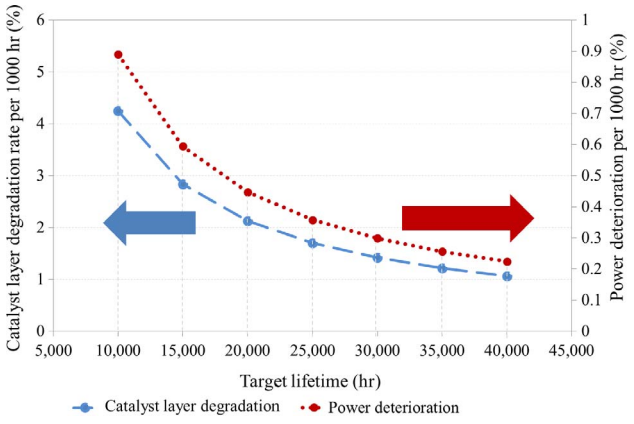

Fig. 13. Catalyst layer degradation and power deterioration rates as a function of target lifetime.

4.4. Optimal operating functions

The DBO model is solved for different target lifetimes and optimum temperature and current density are derived for each target lifetime. Then, discrete optimal points are fit to two curves by regression analysis as presented in Fig. 12. These curves present optimal operating conditions (temperature and current density) as a function of target lifetime.

As presented in Fig. 12, by increasing target lifetime, the decrease in the optimal current density is slower, whereas the optimal temperature decreases consistently. Based on the derived curves, the dependence function of temperature and current density to the target lifetime are determined and presented in Fig. 12.

Fig. 13 shows the optimal output power deterioration and the degradation rate of catalyst layer active surface area as a function of target lifetime. When the target operation life time is 10,000 h, the power deterioration rate per 1000 h is around 0.9% when operating at optimum temperature and current density of 1065.2 K and 2.69 A/cm^2 (derived from Fig. 12). Fig. 12 illustrates that by increasing target lifetime, optimal operating temperature and current density decrease rapidly. Based on the Eqs. (21), (22), nickel oxidation rates is lower at low temperature and current density ranges. The low nickel degradation rate results in lower degradation rate of catalyst layer (Eqs. (23), (24)), and power deterioration consequently. This phenomenon can be seen in Fig. 13. As target lifetime increases, catalyst layer degradation rate and consequently power deterioration falls. When the target operating time is 25,000 h, the performance deterioration is around 0.32% per 1000 h at optimum temperature and current density of 1048.2 K and 2.29 A/cm^2. These results suggest that the operating temperature

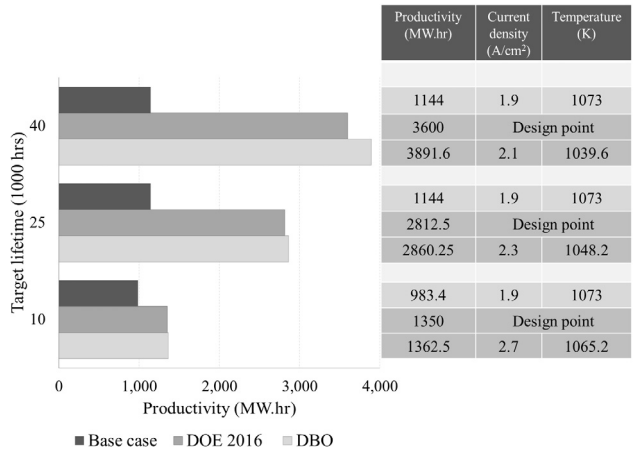

Fig. 14. Comparison of optimal productivity and operating conditions at different target lifetimes for three operation strategies.

and current density should be decreased to achieve lower performance deterioration for long operation but increased if the required lifetime is shorter. This trend is the same for catalyst layer degradation rate as well. As shown in Fig. 13, in accordance with increasing target lifetime, catalyst layer degradation rate decreases and vice versa. It means that increasing the operating temperature and current density is more beneficial for improving the entire performance for brief operation because nickel degradation rate is high in this range of operating conditions and system will not work efficiently for a long duration.

4.5. Comparison

Fig. 14 illustrated the comparison between three operation strategies for the SOFC. Base case strategy optimizes stack operating conditions without considering degradation mechanisms in the optimization procedure. DOE strategy is based on Fuel Cell Multi-Year Research, Development, and Demonstration annual report [39]. According to this report, the performance degradation rate of SOFC stack with stationary application is 2% in 2016, [39]. In addition, the operating lifetime of the cell is between 12,000–70,000 h depending on operating conditions of the system, [39].

The productivity of the SOFC stack operating at different strategies is calculated for different target lifetimes of 10,000, 25,000, and 40,000 h. As can be seen from the figure, DBO model optimum values lead to a more efficient and durable operation of the system than the other operation strategies. Based on the results, at 10,000 h target lifetime, productivities of DBO and DOE strategies are nearly the same and working in DBO operating strategy leads to 27.8% higher power generation in comparison with base case strategy.

As target lifetime increases, the difference between productivities increases. The base case strategy productivity is much lower than two other strategies due to ignoring degradation mechanisms in optimization model. It should be noted that the criterion for cell death is the degradation of half of the nickel. Therefore, system fails after 11,900 h at base case operating strategy and energy generation for both 25,000 and 40,000 h operating time are the same.

However, DOE strategy considers degradation mechanisms in system operation scheduling. This strategy doesn't optimize operating conditions in long term operation and as a result has a lower productivity in comparison with DBO strategy.

5. Conclusion

The performance and degradation of the SOFCs are strongly dependent on the operating conditions (temperature and current density). Thus, it is very important to determine the proper operating conditions to ensure efficient long term operation. The purpose of this paper is to predict the performance and durability of anode supported SOFC and to find the optimal operating conditions for the target operating time. To achieve these objectives, firstly theoretical process module is developed to estimate cell performance. Secondly, degradation module is developed based on the main degradation mechanisms in the anode supported SOFC and the effect of operating conditions on anode catalyst degradation is determined. Moreover, by considering process module in correlation with degradation module, the effect of anode catalyst degradation on performance deterioration is also derived. The results from all developed models corresponded to the experimental data very well. Finally, the optimum operating temperature and current density to satisfy the desired lifetime are found by applying optimization module to the developed process and degradation modules.

Based on the developed DBO model, the optimum temperature and current density as a function of target lifetime are derived to achieve maximum productivity. As a result, at any given target lifetime, the plant operator is enable to implement the optimal operating conditions which maximize system productivity and profitability. Furthermore, to demonstrate the value of DBO framework, system productivity operating at DBO strategy is compared with two other operating strategies. Results demonstrate that the DBO model outputs lead to a more efficient and durable operation of the system compared with the other operation strategies. The suggested methodology is also valuable for commercialization of the anode supported SOFCs.

References

[1] Vialetto G, Rokni M. Innovative household systems based on solid oxide fuel cells for a Northern European climate. Renew Energy 2015;78(1):146–56. http://dx.doi.org/10.1016/j.renene.2015.01.012.
[2] Finsterbusch M. Degradation mechanisms of solid oxide fuel cell cathodes PhD. Thesis Technical University of Frankfurt; 2011http://www.google.com/url?sa=t&rct=j&q=&esrc=s&source=web&cd=3&ved=0CC8QFjACahUKEwjGz6mnuY7HAhUHwxQKHbcuCNA&url=http%3A%2F%2Fwww.db-thueringen.de%2Fservlets%2FDerivateServlet%2FDerivate-24628&ei=XCzAVcaxLoeGU7fdoIAN&usg=AFQjCNEIZqhBQ7GJmOi41mEh0mHtRhydig&sig2=Wr7dKP-nxrwKdd9qa8h6iw&bvm=bv.99261572,d.bGQ.
[3] Suk Joo Bae PHK. Degradation models Technical Report No.123 Atlanta, Georgia, U.S.A.: School of Industrial & Systems Engineering. Georgia Institute of Technology; 2010.
[4] Zhou D, Wu Y, Gao F, Breaz E, Ravey A, Miraoui A. Degradation prediction of PEM fuel cell stack based on multi-physical aging model with particle filter approach. IEEE Trans Ind Appl 2017;53(4):4041–52. http://dx.doi.org/10.1109/TIA.2017.2680406.
[5] Zhou D, Wu Y, Gao F, Breaz E, Ravey A, Miraoui A. Degradation prediction of PEM fuel cell stack based on multi-physical aging model with particle filter approach. Industry Applications Society Annual Meeting, 2016 IEEE, Portland, OR, USA 2016. http://dx.doi.org/10.1109/IAS.2016.7731863.
[6] Zhou D, Gao F, Breaz E, Ravey A, Miraoui A. Degradation prediction of PEM fuel cell using a moving window based hybrid prognostic approach. Energy 2017;138:1175–86. http://dx.doi.org/10.1016/j.energy.2017.07.096.
[7] Parhizkar T, Mosleh A, Roshandel R. Aging based optimal scheduling framework for power plants using equivalent operating hour approach. Appl Energy 2017;205:1345–63. http://dx.doi.org/10.1016/j.apenergy.2017.08.065.
[8] Parhizkar T, Roshandel R. Long term performance degradation analysis and optimization of anode supported solid oxide fuel cell stacks. Energy Convers Manage 2017;133:20–30. http://dx.doi.org/10.1016/j.enconman.2016.11.045.
[9] Roshandel R, Parhizkar T. Degradation based optimization framework for long term applications of energy systems, case study: solid oxide fuel cell stacks. Energy 2016;107:172–81. http://dx.doi.org/10.1016/j.energy.2016.04.007.
[10] Gonzalez JS, Payan MB, Santos JR, Rodriguez A. Maximizing the overall production of wind farms by setting the individual operating point of wind turbines. Renew Energy 2015;80:219–29. http://dx.doi.org/10.1016/j.renene.2015.02.009.
[11] Khalid M, Ahmadi A, Savkin AV, Agelidis AG. Minimizing the energy cost for microgrids integrated with renewable energy resources and conventional generation using controlled battery energy storage. Renew Energy 2016;97:646–55. http://dx.doi.org/10.1016/j.renene.2016.05.042.
[12] Ramadhani F, Hussain MA, Mokhlis H, Hajimolana S. Optimization strategies for solid oxide fuel cell (SOFC) application: a literature survey. Renew Sustain Energy Rev 2017;76:460–84. http://dx.doi.org/10.1016/j.rser.2017.03.052.
[13] Wood AJ, Wollenberg BF, Sheble GB. Power generation operation and control. New York: Wiley-Interscience978-0-471-79055-6; 2013.
[14] Feng H, Chen L, Xie Z, Sun F. Constructal optimization for A single tubular solid oxide fuel cell. J Power Sources 2015;286(1):406–13. http://dx.doi.org/10.1016/j.jpowsour.2015.03.162.

[15] Duhn JD, Jensen AD, Wedel S, Wix Ch. Optimization of a new flow design for solid oxide cells using computational fluid dynamics modelling. J Power Sources 2016;336(1):261–71. http://dx.doi.org/10.1016/j.jpowsour.2016.10.060.
[16] Hasanabadi A, Baniassadi M, Abrinia K, Safdari M, Garmestani H. Optimization of solid oxide fuel cell cathodes using two-point correlation functions. Comput Mater Sci 2016;123(1):268–76. http://dx.doi.org/10.1016/j.commatsci.2016.07.004.
[17] Sadeghi M, Chitsaz A, Mahmoudi SMS, Rosen MA. Thermoeconomic optimization using an evolutionary algorithm of a trigeneration system driven by a solid oxide fuel cell. Energy 2015;89(1):191–204. http://dx.doi.org/10.1016/j.energy.2015.07.067.
[18] Shariatzadeh OJ, Refahi AH, Rahmani M, Abolhassani SS. Economic optimisation and thermodynamic modelling of SOFC tri-generation system fed by biogas. Energy Convers Manage 2015;105(1):772–81. http://dx.doi.org/10.1016/j.enconman.2015.08.026.
[19] Arata Nakajo FM, Brouwer J, Van herle J, Favrat D. Progressive activation of degradation processes in solid oxide fuel cells stacks: Part I: lifetime extension by optimisation of the operating conditions. J Power Sources 2012;216(15):449–63. http://dx.doi.org/10.1016/j.jpowsour.2012.05.078.
[20] Xu M, Li T, Yang M, Andersson M. Solid oxide fuel cell interconnect design optimization considering the thermal stresses. Sci Bull 2016;61(1):1333–44. http://dx.doi.org/10.1007/s11434-016-1146-3.
[21] Prodromidis GN, Coutelieris FA. Thermodynamic analysis of biogas fed solid oxide fuel cell power plants. Renew Energy 2017;108:1–10. http://dx.doi.org/10.1016/j.renene.2017.02.043.
[22] Arata Nakajo FM, Brouwer J, Van herle J, Favrat D. Mechanical reliability and durability of SOFC stacks. Part I: modelling of the effect of operating conditions and design alternatives on the reliability. Int J Hydrogen Energy 2012;37(11):9249–68. http://dx.doi.org/10.1016/j.ijhydene.2012.03.043.
[23] Dimitrova Z, Marechal F. Environomic design for electric vehicles with an integrated solid oxide fuel cell (SOFC) unit as a range extender. Renew Energy May 2017;11. http://dx.doi.org/10.1016/j.renene.2017.05.031.
[24] Aguiar P, Adjiman CS, Brandon NP. Anode-supported intermediate temperature direct internal reforming solid oxide fuel cell. I: model-based steady-state performance. J Power Sources 2004;138(1):120–36.
[25] Wen H, Ordonez JC, Vargas JVC. Single solid oxide fuel cell modeling and optimization. J Power Sources 2011;196(18):7519–32. http://dx.doi.org/10.1016/j.jpowsour.2010.10.113.
[26] Neidhardt JP. Nickel oxidation in solid oxide cells: modeling and simulation of multi-phase electrochemistry and multi-scale transport PhD Thesis Germany: University of Stuttgart; 2013http://elib.uni-stuttgart.de/opus/Ellipsis/Neidhardt_Nickel_oxidation_in_SOC.pdf.
[27] Nehter P. A high fuel utilizing solid oxide fuel cell cycle with regard to the formation of nickel oxide and power density. J Power Sources 2007;164(1):252–9. http://dx.doi.org/10.1016/j.jpowsour.2006.08.037.
[28] Bastien Monnerat LKM, Renken A. Mathematical modelling of the unsteady-state oxidation of nickel gauze catalysts. Chem Eng Sci 2003;58(21):4911–9. http://dx.doi.org/10.1016/j.ces.2002.11.006.
[29] Hardjo DM, Karan K. Numerical modeling of nickel-impregnated porous YSZ-supported anodes and comparison to conventional composite Ni-YSZ electrodes. ECS Trans 2011;35(1):1823–32. http://dx.doi.org/10.1149/1.3570171.
[30] Changrong H, Chen T, Wang WG. The mechanical and electrical properties of Ni/YSZ anode support for solid oxide fuel cells in Anodes. China: Ningbo Institute of Material Technology and Engineering; 2008.
[31] Tanasini P, Cannarozzo M, Costamagna P, Faes A, VanHerle J, Hessler-Wyser A, et al. Experimental and theoretical investigation of degradation mechanisms by particle coarsening in SOFC electrodes. Fuel Cells 2009;9(5):740–52.
[32] Zaccaria V. Gas turbine advanced power systems to improve solid oxide fuel cell economic viability. J Glob Power Propulsion Soc 2017;1:U96IED.
[33] Halinen M. Improving the performance of solid oxide fuel cell systems; 2015.
[34] He Ch, Chen T, Wang WG. The mechanical and electrical properties of Ni/ YSZ anode support for solid oxide fuel cells. Chinese Academy of Sciences, Ningbo Institute of Material Technology and Engineering (NIMTE); 2008. Report No.: A0520.
[35] Odeim F, Roes J, Heinzel A. Power management optimization of an experimental fuel cell/battery/supercapacitor hybrid system. Energies 2015;8(7):6302–27.
[36] Muller A, Weber A, Beie HJ, Krugel A, Gerthsen D, Tiffee E. Influence of current density and fuel utilization on the degradation of the anode. Proc. 3rd Eur Solid Oxide Fuel Cell Forum, Nantes France. 1998.
[37] Singh P, Bansal NP, Ohji T, Wereszczak A. Advances in solid oxide fuel cells IV. John Wiley & Sons; 2009.
[38] Yang SQ, Chen T, Wang Y, Peng Z, Wang WG. Electrochemical analysis of an anode-supported SOFC. Int J Electrochem Sci 2013;8(2):2330–44.
[39] Department of energy, 2016. Annual Report of Fuel Cell Status. https://www.energy.gov/sites/prod/files/2016/06/f32/fcto_myrdd_fuel_cells.pdf.